Disordering of InGaAs/GaAs strained quantum well structures induced by rare gas ion implantation

Sergio Pellegrino, C. Pignataro, Manuela Caldironi, M. Dellagiovanna, F. Vidimari, et al.

Sergio Pellegrino, C. Pignataro, Manuela Caldironi, M. Dellagiovanna, F. Vidimari, Alberto Carnera, A. Gasparotto, "Disordering of InGaAs/GaAs strained quantum well structures induced by rare gas ion implantation," Proc. SPIE 2150, Design, Simulation, and Fabrication of Optoelectronic Devices and Circuits, (2 May 1994); doi: 10.1117/12.175013

SPIE.

Event: OE/LASE '94, 1994, Los Angeles, CA, United States

Disordering of InGaAs/GaAs Strained Quantum Well structures induced by rare gases ion implantation

S.Pellegrino,C.Pignataro,M.Caldironi,M.Dellagiovanna,F.Vidimari
Alcatel-Telettra Research Center
via Trento 30, 20059 Vimercate (Mi), Italy

A.Carnera,A.Gasparotto
Universita' di Padova, Dipartimento di Fisica
via Marzolo 8, 35131 Padova, Italy

Abstract

In this work we have investigated the effect of various implantation schemes on In(0.2)GaAs/GaAs/AlGaAs Single Quantum Well, where the implanted species are Argon and Helium, with doses in the range 1E12 to 1E14 at/cm^2, at energy spanning 270-400 KeV and 30 to 50 KeV for Ar and He, respectively.Repetitive annealing processes were carried out between 735 and 870 °C and the interdiffusion was deduced by photoluminescence measurements.
A maximum of 20 nm shift from He ion implanted Quantum Well with an high degree of reconstruction has been recorded, thus allowing the application of this disordering scheme for the realization of optoelectronic devices.

Introduction

Quantum Well (QW) structures based on III-V compound semiconductors show a remarkable stability respect to constituents interdiffusion.
Typical measured diffusion coefficients at 800 °C for GaAs based Quantum Wells lie arount 1E-18 cm^2/s, leading to diffusion length in the nanometers range for usual thermal treatments.
The QW constituents interdiffusion results in a blue-shift of the electronic transitions induced by the potential profile variation and a net decrease of the concentration of the diffusing constituents (Indium in this case) at the center of the Well.
On the other hand, for device application it is highly desiderable to introduce local variations in the bandgap of the Quantum Wells, and with this technique sophisticated structures like nanostructures [1], lasers integrated with saturable absorbers [2], and others have been realized.
Several techniques have been exploited in order to reduce the thermal stability of the Quantum Well structures, like diffusion induced disordering, impurity free vacancy diffusion, thermal interdiffusion, laser induced intermixing, ion implantation.
The use of ion implantation is particularly interesting since it can have a good lateral definition, the applicability of focussed ion beam allows for the definition of sub-micrometer structures

0-8194-1445-X/94/$6.00

and might be performed with non-doping elements, thus retaining the original doping profile of the epitaxial structure.Till now most of the work was done on AlGaAs/GaAs QW's.Recently the InGaAs/GaAs system was emerging for its high potential use in Optoelectronics, where very low threshold lasers [3], very high frequency modulation [4] and high power [5] devices have been demonstrated.

Experimental

The samples used for intermixing experiments were 7.5 nm In(0.18)GaAs Single Quantum Wells surrounded either by GaAs or by layers of AlGaAs with Al content varying from 20% to 50%, and grown by Low Pressure Metal Organic Chemical Vapor Deposition (LP-MOCVD).
As for the first case, or samples (I), the Quantum Well was grown on (100), 2 deg off toward (110) GaAs substrates and located at 190 nm from the surface.
The second kind of structures, or samples (II) comprises 1.2 microns of Al(0.5)GaAs, 70 nm of Al(0.2)GaAs, 6 nm GaAs spacer symmetrical to the Quantum Well, 70 nm of Al(0.2)GaAs and 100 nm of Al(0.5)GaAs.
The structure was then terminated for protection with a 50 nm GaAs capping layer.The precise structural parameters have been extracted by Transmission Electron Microscopy (TEM) measurements.
The implantation experiments were performed with a 200 KeV Ion Implanter at room temperature, and the samples were tilted 10° respect to the beam axis in order to avoid channeling effects.
The implanted species were Argon and Helium, the energy ranged 270-400 KeV for Ar and 30-50 KeV for He and the doses swept 1E12-1E14 at/cm^2.
The implantation current density was kept as low as 50 nA/cm^2 in order to avoid the effects of dynamical annealing [6], which have been verified by a series of implantation experiments at high current density of 5 μA/cm^2, as shown for comparison with a low current implant in figure 1.It is clearly shown how the maximum strain is higher for the implantation at low current density, since the angular separation of the furthest prominent oscillation from the substrate peak is higher in this later case.

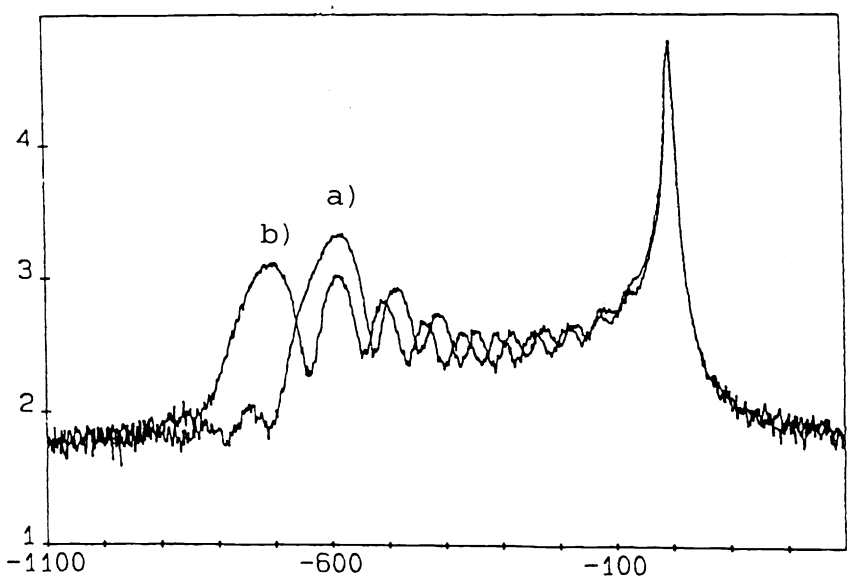

Figure 1:X-Ray Rocking curve of an Argon implanted GaAs substrate at the dose of 1E14 at/cm^2; implantation current density for:
curve a) 5 μA/cm^2
curve b) 50 nA/cm^2

Reconstruction of the damage profile

The implantation process induces crystallographic damage, which can be detected by X-Ray Diffraction (XRD) techniques. The recorded rocking curves are very sensitive to strain profiles which, in case of ion implanted GaAs are positive and perpendicular to the growth surface.The strain was found to be proportional to the density of deposited energy [7], with significant nonlinearities at high implantation doses.
The strain profiles were obtained by iteractive fitting with a dynamical model of diffraction, using vacancy and interstitial distribution of the implanted layers, derived from TRIM-90 code [8], as initial guess of a trial and error procedure.
The damage profile was considered to be linearly related to the strain distribution, and in the calculation the implanted region is divided in thin lamellae uniformly strained.
A reasonably good agreement was usually obtained with five to seven slides, where no significant change was noticed decreasing the discretization step.
In figure 2 we show a measured and simulated rocking curve for an Argon implanted GaAs layer at a dose of 1E14 at/cm^2 and 270 KeV energy. The calculated curve resemble quite closely the

experimental one, allowing for a precise superposition of the implantation-induced damage profile to the Quantum Well location. The simulated XRD rocking curve is very sensitive to small variations of the strain magnitude and position, in fact from the experimental curve also detailed information about the strain profile asymmetry can be extracted.

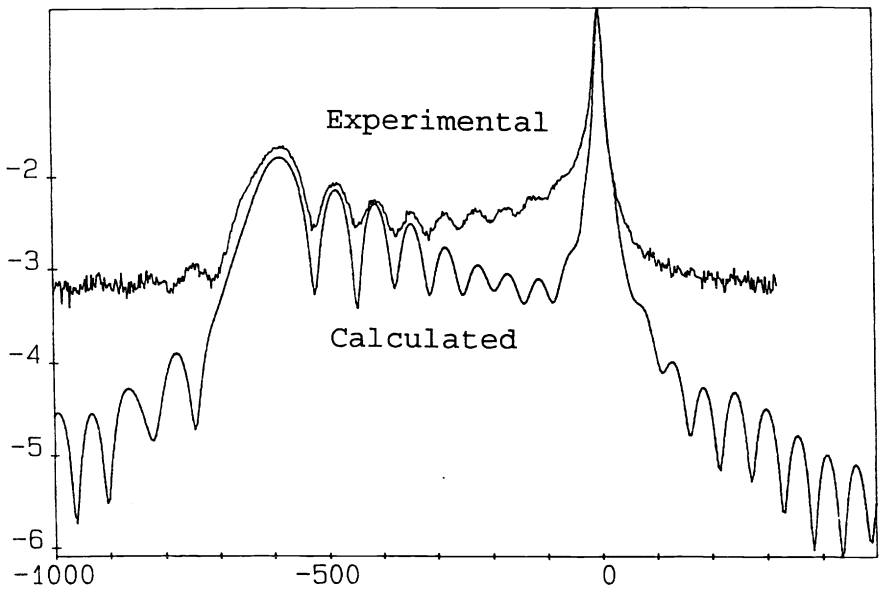

Figure 2:XRD rocking curve for GaAs implanted with Ar at 270 KeV and a dose of 1E14 at/cm^2.

Modelling of the confinement potential for disordered QW

We have considered a Quantum Well of In(x)GaAs/GaAs described in terms of Indium content as follows:
x=0 for $|z| > L/2$ and x=x0 for $|z| < L/2$, where z is the growth direction, L is the well width, and then the confinement profile is ideally rectangular.In the simple approximation of Fickian diffusion of atomic species, from two semi-infinite barriers with the well of width L centered at z=0, the resulting distribution of Indium, following an high temperature annealing process, is given by:

$$x(z)=x0*(0.5*\mathrm{erf}[(z+L/2)/2*\Delta] - 0.5*\mathrm{erf}[(z-L/2)/2*\Delta]) \quad [1]$$

where x0 is the initial indium molar fraction and Δ is the diffusion length.
The profile of the molar fraction x of Indium in the growth direction, and the corresponding confinement potential for the electron-hole pairs it is not more rectangular, the Quantum Well

shape is enlarged and, more important, the maximum Indium concentration, localized at the center of the well might be significantly lower than its initial value.This results in a local increase of bandgap of the Quantum Well and then a blue-shift of the recombination wavelength from the fundamental electron-hole levels.Given the x profile, the corresponding energy gap profile is obtained from the following:

$$Eg(x)=Eg0(x)+ dEh(x) \ -/+dEs(x) \qquad [2]$$

where -/+ account for heavy-holes and light-holes, respectively, E0=1.424-1.53x+0.45x^2 [9] is the unstrained bulk material, dEh is the hydrostatic contribution of the strain, and dEs is the heavy-hole, light-hole splitting induced by the strain.
Clearly all the parameters are dependent on Indium molar fraction, and the values are linearly interpolated from the binary values.It was assumed in the calculation that dEc=62% and dEv=38% [9].
In order to calculate in the Envelope Function formalism, for an arbitrary potential profile, the confinement energy for electrons and holes we have used the Transfer Matrix Method (TMM) [10]; in such a formalism the potential profile along the growth direction has been divided in N intervals where the potential is assumed to be constant.The extrema are taken as semi-infinite and correspond to the GaAs barriers, while the others have a monolayer thickness.
The envelope function in a given interval (j) is

$$Xj=(z,E)=Aj*\exp[iKj(z-z(j-1))]+Bj*\exp[-iKj(z-z(j-1))] \qquad [3]$$

where mj and Vj are the effective mass and potential in the interval, respectively, and the constants are defined by the boundary conditions of continuity of X and its derivative, at the interface z(j-1)

$$\begin{bmatrix} Aj \\ Bj \end{bmatrix} = Mj \begin{bmatrix} A(j-1) \\ B(j-1) \end{bmatrix} \qquad [4]$$

where Mj is a 2*2 transfer matrix.
By repeatitive iteration at every interface, one obtains the following relation between the coefficients of the envelope function at the extrema j=0 and j=N-1

$$\begin{bmatrix} A\ (N-1) \\ B\ (N-1) \end{bmatrix} = M \begin{bmatrix} A1 \\ B1 \end{bmatrix} \qquad [5]$$

where M is the product of the tranfer matrix at the various interfaces.
The condition for bound states, vanishing wavefunction at +/- ∞, is satisfied when M22=0, and then the eigenvalues E are the zeros of the matrix element M22.

Results and discussion

Helium implantation

Photoluminescence measurements were performed on as grown samples (II), resulting in a wavelength emission at λ=975 nm at 300 K and λ=917 nm at 8K.The good optical quality of the starting materials was prooved by a Low Temperature (LT) photoluminescence FWHM of 5 meV.
He implantation experiments at dose of 1E14 at/cm^2 were performed at 30,38 and 50 KeV.The choice of the three implantation energies was based on TRIM simulation, in order to set the maximum of the implantation damage at a damage standard deviation from the Quantum Well, at the Quantum Well position and to a damage standard deviation beyond the Quantum Well.The subsequent annealing process was done at the temperature of 870 °C, in Arsenic overpressure, lasting 10 minutes.
The photoluminescence measurements gave prominence to significant blue-shift of the emission wavelength, both on reference annealed and on ion implanted annealed samples.In table 1 are summarized the results obtained on He implanted samples.

SAMPLE	λ(nm)	Δ^2 ($10^{-16}cm^2$)	D (cm^2/sec)
Reference Sample	975	n.a.	n.a.
Annealed Reference Sample	956	230	3.8E-17
Implanted @ 30 KeV Annealed	945	430	n.a.
Implanted @ 38 KeV Annealed	938	600	n.a.
Implanted @ 50 KeV Annealed	939	580	n.a.

Table 1:PL peak wavelength, squared diffusion length, and diffusion coefficient for the He implanted samples (II).

The reference annealed samples exhibit a blue-shift of about 20 nm, meaning that the interdiffusion mechanism is already playing a major role.By the TMM alghoritm we computed the diffusion length, in order to derive the recombination at 956 nm.In table 1 is reported the inferred diffusion coefficient for the reference annealed sample, which is in good agreement with the value reported in [11].In order to confirm the excellent agreement with litterature data, lower temperature thermal treatments have been performed with different Arsenic overpressure.
The experiments were perfomed in a LP-MOCVD reactor at 735 °C with either 50 sccm or 200 sccm arsine flow, without detecting noticeable differences among the two cases.
In this case the peak wavelength was 969 nm and the corresponding calculated diffusion coefficient was D=3.3E-18, a value to be compared with D=2.4E-18, as derived from reference [11].
It appears then that the Quantum Well, in samples (II), is located beyond the diffusion length of vacancies, rendering the In/Ga interdiffusion process almost indipendent from the vapour phase composition.We have also detected a noticeable reduction of the FWHM in the reference annealed samples, as shown in figure 3, with a minimum linewidth of about 3.5 meV for the annealing process at 870 °C.

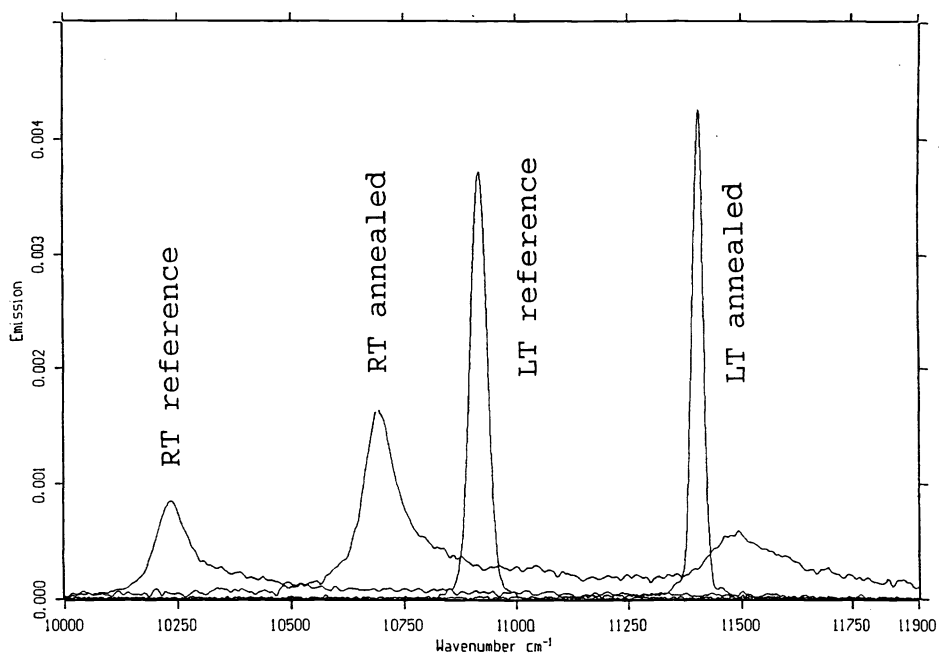

Figure 3:RT and 8K spectra for reference and reference,annealed samples (II): a linewidth narrowing to 3.5 meV is detected for the reference,annealed sample.

As for the implanted and annealed samples, in table 1 are reported the measured emission wavelength and the calculated diffusion

lengths.A qualitatively good agreement of the wavelength shift at different implantation energies is found, even if the bell-like profile of the shift is less symmetryc than expected.From this data it appears that the damage profile location, as derived by TRIM simulation, is overestimated and the actual Quantum Well location should lie between the damage profiles created by the 38 and 50 KeV implantation processes.In figure 4 are shown for comparison the photoluminescence spectra of the reference and 50 KeV implanted and annealed samples.It has to be noticed that the PL intensity is comparable, indicating that the thermal process is adeguate to recover the crystal quality.
On the contrary, the anneling processes performed at 735 °C (up to one hour), have shown a very little reconstruction degree of the lattice, leading to a poor PL emission intensity.

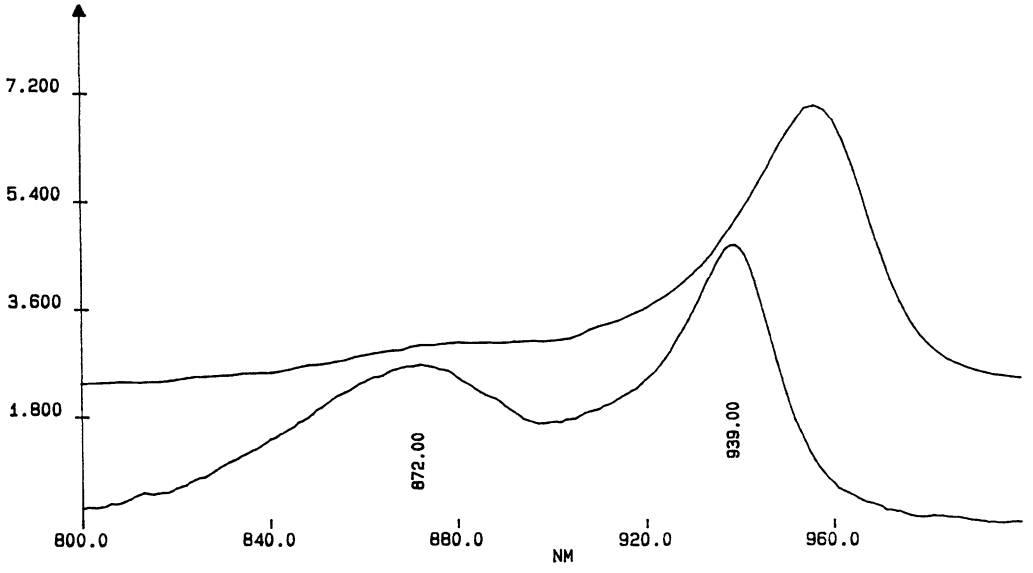

Figure 4:RT photoluminescence spectra of reference (upper curve) and 50 KeV implanted,annealed (lower curve) samples (II).

Argon implantation

Samples (I) were implanted with Ar at 270, 350, and 400 KeV, and doses from 1E12 to 1E14 at/cm^2.
Thermal annealing processes carried out on Ar implanted samples (I) result in low reconstruction degree, with an anomalous associated shift of the annealed reference respect to samples (II) and letterature data.Table 2 summarizes the ensemble of the experiments and underlines the anomalous behaviuor of the annealed samples.

Annealing Conditions	Implantation Energy (KeV)	Implantation dose (at/cm^2)	λ(nm)
Reference			980
735 °C 60 min.	Reference		963
	270	1E12	974
		1E13	970
	350	1E12	973
		1E13	979
	400	1E12	967
870 °C 10 min.	Reference		935
	270	1E12	935
		1E13	952
		1E14	947

Table 2:PL peak wavelength for the Ar implanted samples.

In most cases the annealed reference sample show a blue-shift which is:
a) larger than expected from letterature data [11]
b) larger than the reference annealed samples (II) treated in the same conditions
and
c) larger than the Ar implanted samples
We tentatively explain these results as follows: it is known that the use of encapsulants like silica result in an induced intermixing through Ga vacancies injection in the Quantum Well, and that this effect is reduced in case of use of Silicon nitride capping.
A recent observation of enhanced intermixing in InGaAs/GaAs system has been recently explained by W.P.Gillin et al. [12] through the same mechanism, even if the capping and annealing conditions used in their work look unfavourable to magnificate this effect.The calculated diffusion length of Gallium vacancies at the high temperature annealing condition is about 250 nm, deeper than the Quantum Well location.
Then the lower thermal stability found in our samples might be tentatively explained with a strong interaction with the surface to enhance the vacancy/interstitial concentration at the QW, thus increasing the effective In/Ga diffusion coefficient.

Since in samples (II) no anomalies have been found, we expect that the grup III vacancy diffusion length in these structures is significantly lower than the one estimated for structures (I).
The question remains completely open in case of the implanted samples, where the damaged region might profoundly disturb the interaction with the surface.Further work is needed to clarify these points.

Conclusions

A methodological work has been carried out on Ar and He ion implanted on single Quantum Well structures (I) and on laser-like samples (II).The damage profile was reconstructed via XRD analysis and simulation, using TRIM-code computed vacancy distribution as initial guess of the trial and error procedure.
A precise location of the QW position respect to the damage profile was possible and the scheme was applied to He implantation at 30,38 and 50 KeV.High degree of reconstruction has been detected following 870 °C annealing process, with a maximum of about 20 nm blue-shift respect to the annealed reference samples.These characteristics render the process appealling for application to optoelectronic device technology.

Acknowledgement

We are deeply indebt to Dr.C.Frigeri, MASPEC Parma, for TEM measurements and to Dr.A.DiPaola for continuous help during the work.

References

[1] C.Vieu,M.Schneider,D.Mailly,R.Planel,H.Launois,J.Y.Marzin, and B.Descouts, "Optical characterization of selectively intermixed GaAs/GaAlAs quantum wires by Ga+ masked implantation," J.Appl.Phys. 70 (1991) p.1444
[2] N.Yamada, and J.S.Harris,Jr., "Strained InGaAs/GaAs single quantum well lasers with saturable absorbers fabricated by quantum well intermixing," Appl.Phys.Lett. 60 (1992) p.2463
[3] T.R.Chen,L.E.Eng,B.Zhao,Y.H.Zhuang, and A.Yariv, "Strained single quantum well InGaAs lasers with a threshold current of 0.25 mA," Appl.Phys.Lett. 63 (1993) p.2621
[4] J.D.Ralston,S.Weisser,E.C.Larkins,I.Esquivias,P.J.Tasker, J.Fleissner, and J.Rosenzweig, "Modulation bandwidths up to 30 GHz under CW bias in Strained In.35GaAs/GaAs MQW lasers with p-doping," Post deadline paper PD-5, 13th International Semiconductor Laser Conference, 1992 Takamatsu, Japan
[5] T.R.Chen,L.E.Eng,Y.H.Zhuang,Y.J.Xu,H.Zaren, and A.Yariv, "High-power operation of buried-heterostructure

strained-layer InGaAs/GaAs single quantum well lasers," Appl.Phys.Lett. 57 (1990) p.2762
[6] T.E.Haynes, and O.W.Holland, "Dose rate effects on damage formation in ion-implanted gallium arsenide," Nucl.Instr. and Meth. B59/60 (1991) p.1028
[7] B.M.Paine,N.N.Hurvitz, and V.S.Speriosu, "Strain in GaAs by low-dose ion implantation," J.Appl.Phys. 61 (1987) p.1335
[8] J.Ziegler, Ion Implantation: Science and Technology, Academic Press, New York, 1988
[9] D.J.Arent,C.Van Hoof,G.Borghs, and H.P.Meier "Heterojunction band discontinuities for pseudomorphically strained InxGaAs/AlyGaAs heterointerfaces," on Condensated Systems of Low Dimensionality, NATO ASI series 1991, p.547
[10] B.Jonsson, and S.T.Eng, "Solving the Schroedinger equation in arbitrary Quantum-Well potential profiles using the Tranfer Matrix Method," IEEE J-QE 26 (1990) p.2025
[11] F.Iikawa,P.Motisuke,J.A.Brum,M.A.Sacilotti,A.P.Roth, and R.A.Masut, "Thermally induced In/Ga interdiffusion in InxGaAs/GaAs strained single Quantum Well grown by LPMOVPE," J.Crystal Growth 93 (1988) p.336
[12] W.P.Gilling,D.J.Dunstan,K.P.Homewood,L.K.Howard, and B.J.Sealy, "Interdiffusion in InGaAs/GaAs quantum well structures as a function of depth," J.Appl.Phys. 73 (1993) p.3782.